

# Wavelet Based Image Registration of Radiometrically Corrected Satellite Images

Miss Heena Patel\*  
Mr. Ashish Srivastava\*\*  
Mr. R. M. Parmar\*\*\*  
Dr. Vipul Shah\*\*\*\*

## Abstract

This Paper investigates the use of Wavelets for automatic registration and for onboard processing of remote sensing satellite imagery. The zero tree structure of the wavelet coefficients provides a unique and fast method to predict the location of the control points in a hierarchical fashion. This approach reduced the search space for determining the control points required for image registration. Considering the computation intensive and memory intensive characteristics of remote sensing image registration and the limited computing power of onboard hardware to implement image registration efficiently and effectively with dedicated architecture is of great significance. Due to excellent reconfigurability and convenient design flow, FPGA is proposed for a fast automatic image registration.

**Keywords :** Radiometrically Correction, Satellite Image Processing, Wavelet Transformation, Image Registration, FGPA, Image Reconfiguration.

## 1. Introduction

### 1.1 Background

Typically, registration is applied in remote sensing (multispectral classification, environmental monitoring, change detection, weather forecasting, creating super-resolution images, integrating information into geographic information systems (GIS)), in medicine (combining computer tomography (CT) and NMR data to obtain more complete information about the patient, monitoring tumor growth, treatment verification, comparison of the patient's data with anatomical atlases), and in computer vision Image registration methodology. It is the process of overlaying two or more images of the same scene taken at different times, from different viewpoints, and/or by different sensors. It geometrically aligns two images—the reference and sensed images as shown in figure 1.

Any remote sensing image, regardless of whether it is acquired by a multispectral scanner on board a satellite, a photographic system in an aircraft, or any other platform/sensor combination, will have various geometric distortions [1]. In satellite Technology, there is lot of development going on to design and develop micro satellites, which provide multi spectral imagery, but are limited in bandwidth and power. So there is requirement of suitable compression technique for data transmission.

Similarly in high resolution satellites, data rate is tremendous requiring large compression ratio. Due to inherent property of compression systems which modify pixel values so as to make them dependent on adjacent pixels, the corrections like radiometric and geometric have to be implemented before image compression for better image quality with better SNR. It is also found that this preprocessing is mandatory for higher compression ratios, in order to avoid degradation of the image due to loss in compression. With the rapid innovations of hardware technology like FPGA, microprocessor and microcontrollers, more and more image processing algorithms are enforced to be finished onboard instead of at ground station to meet the requirement of processing numerous remote sensing data real timely [10]. Our work is basically a study of wavelet based image registration and as a proof of this concept we present simulation results of our algorithm.

## 2. Image Registration Steps

In conventional image registration, any new incoming sensed image is going to be registered relative to a known reference image, by following four steps [2]:

- a) **Feature space** :- the image features extracted from reference and sensed images. These features may include edges, contours, or high-interest points.
- b) **Search space** :- the class of potential transformations that establish the correspondence between input data and reference data. Typical transformations are rigid, affine, and polynomial.
- c) **Search strategy** :- the procedure selected to estimate the transform parameters. Common search strategy includes local or global, hierarchical or multiresolution.
- d) **Similarity metric** :- evaluates the match between input data and reference data for a given transformation chosen in the search space. These steps are elaborated in the following sections.

### 2.1 Feature space

The geometric registration process involves identifying the image coordinates (i.e. row, column) of several clearly discernible points, called ground control points (or GCPs), in the distorted image, and matching them to their true positions in ground coordinates (e.g. latitude, longitude). In order to determine the geometrical relationship between the images, it is necessary to extract tie points or ground control points(GCP) from each image. The objective of this step is to reduce both images into point data sets. These control points are used to compute the specific transform coefficients.

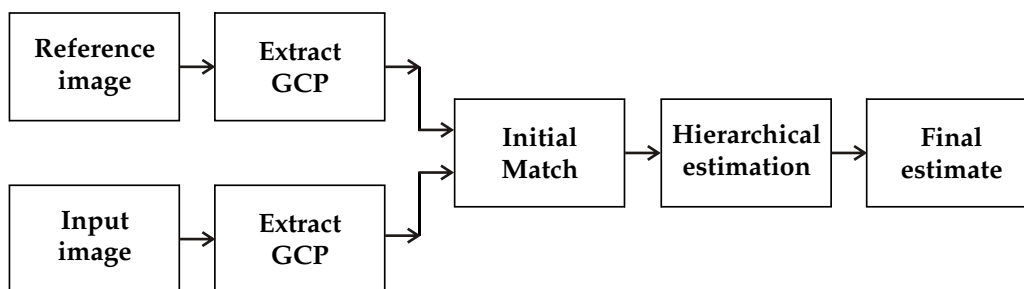


Fig.1 Block Diagram of basic Image registration

### (i) Control Point Extraction:

As the manual identification of control points may be time-consuming, tedious, and not feasible in the hardware implementation, so automated techniques have been developed. Our approach to automatic registration algorithms uses the Laplacian of Gaussian (LoG) operator to automatically extract ground control points from the images as shown in figure 2. The input image is filtered with the LoG operator and thresholded to extract the extrema points. These points represent areas within the image that exhibit high rates of variation and should be semi-invariant for like images that have been acquired under similar viewing conditions. This technique has been demonstrated robustly against multisensor and multispectral datasets with similar spatial frequency content (edge information). The filter kernel for the LoG is given by,

$$\begin{bmatrix} -1 & -2 & -1 \\ -2 & 12 & -2 \\ -1 & -2 & -1 \end{bmatrix}$$

The LoG output image is threshold according to the following,

$$B(x,y) = \begin{cases} 1, & |L(x,y)| \geq q*s \\ 0, & \text{else} \end{cases}$$

Where s is the standard deviation of L(x,y) and q is a constant (q ∈ [1]). The value of q determines the number of extrema points extracted from the image. The point sets can be sorted and truncated to a predetermined size based on the desired speed of the point matching and processing limitations. After GCP identification, control point matching algorithm is used to match corresponding pairs of points.

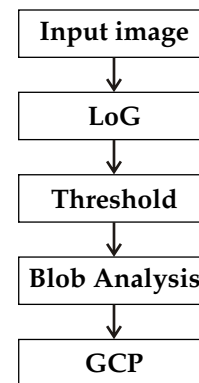


Fig.2 Ground Control point Extraction scheme

### (ii) Control Point Matching

The accuracy of the registration depends on the success of dissimilar point sets. In this algorithm, dual-matching criteria is applied, which are distance matching and cross-correlation as shown in figure 3. The two rows that have the greatest number of distance matches are considered matched points. A point is considered a match if  $d > T_d$ , where  $T_d$  was determined by,  $T_d = 0.5 \max \{N_r, N_s\}$ .

where  $d$  is the number of matches,  $T_d$  is the threshold value and  $N_r$  and  $N_s$  are the number of points in the reference and sensed point data set.

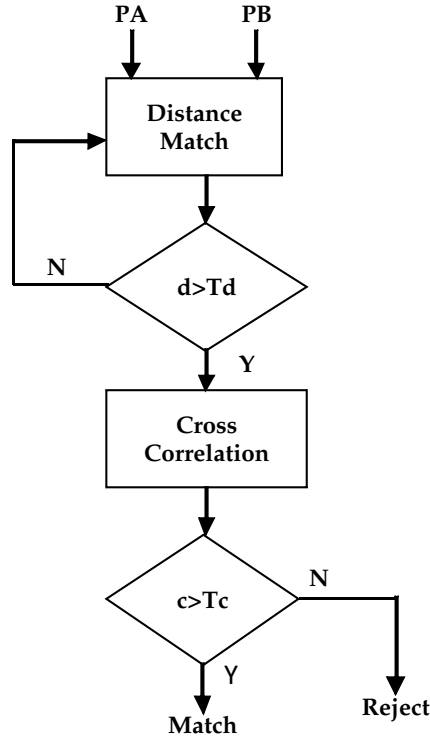


Fig.3 Point Matching Scheme

The cross correlation is known to produce successful matching results. The disadvantage of the method is the computational burden associated with computing the correlation and the detrimental effects of comparing images with high degrees of rotation without a priori knowledge. We reduce this burden by computing the correlation over a small window and on a limited number of points. Only the points that pass the distance criteria are used to compute the cross-correlation. The cross-correlation over a  $(2w+1) \times (2w+1)$  window is defined as,

$$c(i, j; k, l) = \frac{\sum_{q=-w}^w \sum_{r=-w}^w (I(i+q, j+r) - \mu_R) \cdot (I(k+q, l+r) - \mu_S)}{\left[ \sum_{q=-w}^w \sum_{r=-w}^w (I(i+q, j+r) - \mu_R)^2 \right] \left[ \sum_{q=-w}^w \sum_{r=-w}^w (I(k+q, l+r) - \mu_S)^2 \right]} \quad (1)$$

Where  $I_R$  is the reference image,  $I_S$  is the sensed image, and  $\mu_R$  and  $\mu_S$  are the mean of the analysis window in the reference and sensed image, respectively. The cross-correlation is used to confirm the points are located in the same image area. In our work,  $w=1$  and a point is considered a match if  $c > 0.75$ .

### 2.4 Search space and strategy

In this step optimum transform and its parameters are computed. Affine transforms is commonly used for geometric correction of remote sensing images. 2-D affine transformation model is defined by

$$\begin{bmatrix} x \\ y \end{bmatrix} = s \begin{bmatrix} \cos\theta & \sin\theta \\ -\sin\theta & \cos\theta \end{bmatrix} \begin{bmatrix} X_r \\ Y_r \end{bmatrix} + \begin{bmatrix} t_x \\ t_y \end{bmatrix} \quad (2)$$

Where  $\theta$  represents the rotation  $(t_x, t_y)$  denote the translation in the  $x$ - and  $y$ - direction and  $s$  denotes the scale. The affine transformation maps the reference coordinates,  $(x_r, y_r)$ , into the sensed coordinates  $(x, y)$ . For the remainder of

our analysis, we assume the scale,  $s=1$ . Thus, we can express above equation as

$$\begin{bmatrix} x \\ y \end{bmatrix} = \begin{bmatrix} f(x_r, y_r) \\ g(x_r, y_r) \end{bmatrix} = \begin{bmatrix} u & v \\ -v & u \end{bmatrix} \begin{bmatrix} x_r \\ y_r \end{bmatrix} + \begin{bmatrix} t_x \\ t_y \end{bmatrix} \quad (3)$$

Where  $u = \cos \theta$ ,  $v = \sin \theta$  and the model parameters are given by  $\psi = (u, v, t_x, t_y)$ .

We define the error term as

$$\epsilon^2 = (x - f(x_r, y_r))^2 + (y - g(x_r, y_r))^2 \quad (4)$$

The model parameters can be estimated by minimizing the function

$$J = \sum_{i=1}^N \epsilon_i^2 \quad (5)$$

Where  $N$  is the number of matched points or GCPs. The solution of (5) is obtained by least square techniques. The estimated parameters  $\psi = (u, v, t_x, t_y)$  are used to register the images.

### 2.5 Similarity Metric

This step is used to determine to optimal match between corresponding images. Commonly used methods are correlation measures, distance measures, and statistical measures [2]. Algorithm is similar to as mentioned in control point matching.

Drawback with conventional method is searching of large space for control point extraction affecting the speed of total registration process. Wavelet based image registration reduces the computing time and increases the robustness of the algorithms. The structural properties of the wavelet coefficients can be exploited in a unique fashion to reduce the search space for the control points. The main advantage of this approach is its ease of implementation on high-performance parallel computing and registering large image data sets because full size does not require processing.

## 3. Wavelet Based Image Registration

In the proposed wavelet based registration, the reference and sensed images are decomposed with the DWT as shown in Figure 4. Since the LL-band retains most of the image information, each LL-band is processed to extract the control points. The control points are generated using the conventional method to obtain an initial match at the lowest resolution level,

R0. These points serve as estimates for the control points at higher resolutions, which are refined in the high frequency bands (LH, HL, HH). This eliminates the need to detect control points at higher resolutions and greatly increases processing efficiency, ultimately allowing for the registration prediction of extremely large images. A hierarchical estimation procedure is implemented to determine the transform parameters [5]. The zero tree structure is used to identify control points in the same frequency band but at different resolutions.

**3.1 Zero-tree prediction**

The zero tree prediction approach provides an estimate to the location of the control points from resolution level  $R_{k-1}$  to  $R_k$ . Let  $(i, j)$  and  $(m, n)$  denote a matched pair between the reference and sensed images at resolution  $R_{k-1}$ . Denote the set of points generated from the zero-tree relation as

$$Oa(i,j)=\{(2i,2j),(2i-1,2j),(2i,2j-1),(2i-1,2j-1)\} \tag{6}$$

$$Ob(m,n)=\{(2m,2n),(2m-1,2n),(2m,2n-1),(2m-1,2n-1)\} \tag{7}$$

Where  $Oa$  and  $Ob$  represent the set of points in the reference and sensed images. The points  $(2i, 2j)$  and  $(2m, 2n)$  serve as predicted matched points at resolution  $R_k$ . This match is updated by computing the cross correlation between corresponding points given by,

$$C1 = c(2i, 2j; 2m, 2n), \tag{8}$$

$$C4 = c(2i-1, 2j-1; 2m-1, 2n-1). \tag{9}$$

The maximum value of the correlation coefficients is given by,  $C_{max} = \max\{C1...C4\}$ . The point pair that yields the maximum value,  $C_{max}$ , is selected as the best match.

**3.2 Hierarchical Estimation Approach**

This is used to find the transform parameters. Let the set of matched points for the reference and sensed images for  $R_0$  be denoted as  $\{A_0\}$  and  $\{B_0\}$  respectively. These points results due to matching procedure from the LL bands of each image. Starting with  $R_1$ , the set of match points for each subband (LH1, HL1, HH1) is given by;

$$A1_{(i,j)} = \begin{cases} A_0(i, j + H_b) \text{ for } LH_1 \\ A_0(i + W_b, j) \text{ for } HL_1 \\ A_0(i + W_b, j + H_b) \text{ for } HH_1 \end{cases} \tag{10}$$

$$B1_{(m,n)} = \begin{cases} B_0(m, n + H_b) \text{ for } LH_1 \\ B_0(m + W_b, n) \text{ for } HL_1 \\ B_0(m + W_b, n + H_b) \text{ for } HH_1 \end{cases} \tag{11}$$

Where  $W_b \times H_b$  denote the width and height of the wavelet subband. For each wavelet subband, the transform parameters are estimated for  $R_1$  resulting in  $\Psi = (u_1, v_1, t_{x1}, t_{y1})$ . The subband producing the estimate with the minimum error is selected as the best estimate for  $R_1$ . Similarly calculate parameters at each resolution (1..L). The transform parameters at  $R_L$  (highest subband) are interpreted to obtain the parameters for full size image.

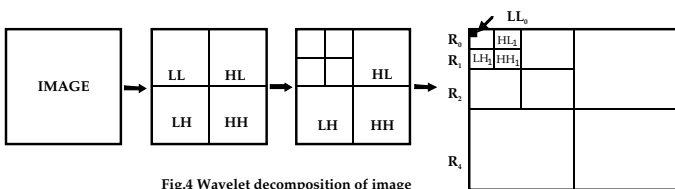
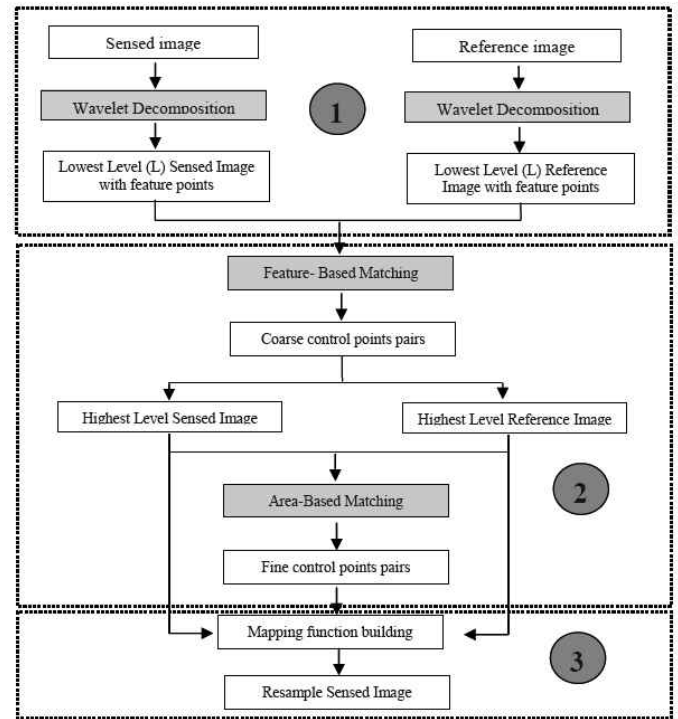


Fig.4 Wavelet decomposition of image

**4. Study on Test Images**

The simulations were carried out by both conventional and wavelet based registration methods. Both are giving the same level of registration but conventional method is with more complex computations. In this section wavelet based results have been shown. Figure 5 shows the basic steps as follows:

- (a) Wavelet decomposition of reference image.
- (b) Wavelet decomposition of sensed image.
- (c) Find maxima of LH & HL coefficients for each level of decomposition starting from the lowest level and iteratively refine maxima points (GCPs).
- (d) The best transformation is iteratively refined and applies on sensed image by suitable transformation
- (e) Resample the sensed image.



**4.1 Simulations**

The basic image is a 366 X 365 section of an image westconcord orthophoto supplied by Massachusetts geographic information system. The image is manually rotated and distorted by scale  $\{\theta, s\}$  to observe the performance of the algorithm. The westconcordortho photo image was transformed by  $\{30, 0.6\}$ . In table the estimated parameters values  $\{\theta, s\}$  are shown at each resolution levels,  $R_k$ , and each wavelet subband  $LH_k, HL_k, HH_k$  for  $k=1, \dots, 3$ .

## i) WAVELET Decomposition of Sensed Image And Reference Image

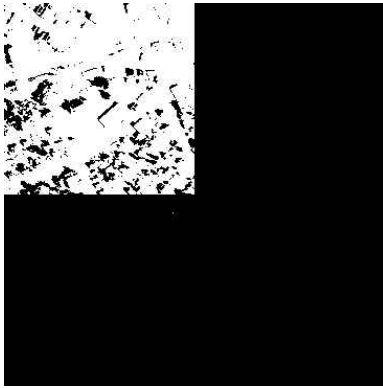


Fig. 6 Wavelet Decomposition of Reference Image

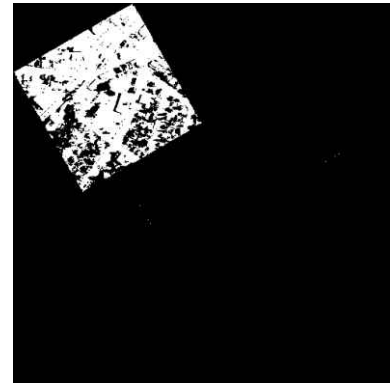


Fig. 7 Wavelet Decomposition of Sensed Image

## ii) Automatic GCPs Selection



Fig. 8 Ground Control Point Selection for Reference image

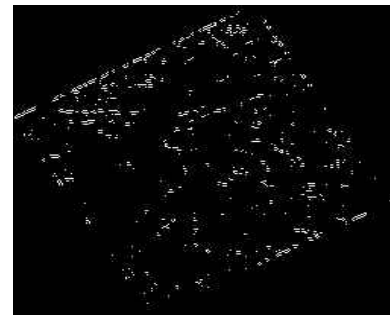


Fig. 9 Ground Control Point Selection for Sensed image

## iii) Angle and Scale recovery at Different Resolution level

Decomposition levels/approximation or detail	Angle Recovery	Scale Recovery
cA1(Approximation level-1)251X251	30.4457	0.3013
CH1(Horizontal level-1) 251X251	30.3181	0.3023
cV1(Vertical level-1) 251X251	30.3502	0.3028
cD1(Diagonal level-1) 251X251	31.2502	0.3009
cA2(Approximation level-2)126X126	30.1957	0.1521
CH2(Horizontal level-2) 126X126	29.9546	0.1519
cV2(Vertical level-2) 126X126	31.3578	0.1517
cD2(Diagonal level-2) 126X126	29.8833	0.1519
cA3(Approximation level-3)63X63	30.5567	0.0756
CH3(Horizontal level-3) 63X63	30.6144	0.0753
cV3(Vertical level-3) 63X63	30.6628	0.0756
cD3(Diagonal level-3) 63X63	30.0461	0.0750
cA4(Approximation level-4)32X32	30.2462	0.0381
CH4(Horizontal level-4) 32X32	30.0408	0.0377
cV4(Vertical level-4) 32X32	30.1416	0.0381
cD4(Diagonal level-4) 32X32	30.5982	0.0367

## OUTPUT:



Fig 10 Sensed Image



Fig.12 Recovered image



Fig.11 Rerence image



Fig 13 Residue image

In the algorithm from lower to higher resolution the control points are iteratively refined and registration becomes faster, accurate and efficient. Different Transforms were also applied, but Affine transform gives better results with low residue error.

## 5. Conclusion and Future Work

For reasons of speed, portability, and accuracy, automatic wavelet based georegistration is an important requirement to ease the work load, speed up processing, and improve the accuracy in locating a sufficient number of well-distributed accurate tie points (GCPs). The Wavelet multiresolution processing of the image data provided an efficient method for registering large image data sets because the full-size image was not processed. Search strategy using wavelet enables reductions in computing time and increases the robustness of the algorithms. Matching is done globally over the image, instead of locally for each pair of CPs. One of the main advantages of this approach is its ease of implementation on high-performance parallel computing [6]. Due to reconfigurability and design flow FPGA has been most preferably used for image registration especially in medical imaging [9].

## 6. References

1. L. Brown, "A survey of image registration techniques," *ACM Computing Surveys*, vol. 24, no. 4, pp. 325–376, 1992.
2. B. Zitova and J. Flusser, "Image registration methods: a survey," *Image and Vision Computing*, vol. 21, no. 11, pp. 977– 1000, 2003.
3. J.-P. Djamdji, A. Bijaoui, and R. Maniere, "Geometrical registration of images: the multiresolution approach," *Photogrammetric Engineering & Remote Sensing*, vol. 59, no. 5, pp. 645–653, 1993.
4. J. LeMoigne, W. J. Campbell, and R. F. Crompt, "An automated parallel image registration technique based on the correlation of wavelet features," *IEEE Transactions on Geoscience and Remote Sensing*, vol. 40, no. 8, pp. 1849–1864, 2002.
5. J. Le Moigne and I. Zavorin, "Use of wavelets for image registration," in *Wavelet Applications VII*, vol. 4056 of *Proceedings of SPIE*, pp. 99–104, Orlando, Fla, USA, April 2000.
6. A. El-Ghazawi and P. Chalermwaa, "Wavelet-based image registration on parallel computers," in *Proceedings of ACM/IEEE on High Performance Networking and Computing (SuperComputing '97)*, p. 20, 1997.
7. H.Li, B.S.Manjunath, and S.K.Mitra, "A Contour-Based Approach to Multisensor Image Registration" *IEEE Trans. Image Processing* Vol.4(3), pp.320-334, 1995.
8. S. T. Bamard and W. B. Thompson, "Disparity analysis of images," *IEEE Trans. Pattern Anal. Mach. Intell.*, vol. PAMI-2, pp. 333-340, Feb. 1980.
9. Baofeng Li, Yong Dou, Haifang Zhou, and Xingning Zhou, "FPGA Accelerator for Wavelet-Based Automated Global Image Registration", *EURASIP Journal on Embedded Systems* Volume 2009.
10. V.Kalyana Sundaram, K.Thenmozhi Selvi, M.Vanitha and S.R.Nagraj, "Onboard Realization for Radiometric Pre-processing for 'Le-Gall' Wavelet Filter Based Compression", *Journal of Spacecraft Technology*, Vol.18, No-2, pp.27-41, July 2008
11. *Fundamentals of Remote Sensing* by Jeorge Joseph [12] *Digital Image Processing* by Rafael C. Gaunzaleuz and Richard E. Woods